

Simulation of Shock Wave Structure in Nitrogen with Realistic Rotational Spectrum and Molecular Interaction Potential

F.G. Tcheremissine, V.I.Kolobov and R.R.Arslanbekov

*Dorodnicyn Computing Center of the Russian Academy of Sciences,
119991, Moscow, Russia, tcherem@ccas.ru
CFD Research Corporation,
Huntsville, AL, USA, vik@cfdr.com*

Abstract. The shock wave structure in nitrogen is studied by solving the Boltzmann kinetic equation generalized for polyatomic gases with internal degrees of freedom. The collision operator is evaluated by the method proposed in [1, 2] that ensures strict conservation of mass, impulse and energy and gives equilibrium rotational spectrum at the thermodynamic equilibrium conditions. Detailed distributions of gas density, translational and rotational temperatures are presented together with populations of the rotational levels at several characteristic points along the shock wave front. Non-equilibrium rotational spectrum is obtained inside the shock wave. Results of simulations are compared to experimental data and simulation results of other authors obtained by Monte Carlo methods

Keywords: Shock Wave Structure, Polyatomic Gas, Boltzmann Equation, Rotational Spectrum

PACS: 51.10+y, 05.20Dd

INTRODUCTION

Numerical study of the shock wave structure in a polyatomic gas with rotational degrees of freedom presents interest by two main reasons. First, it provides additional data about the process of rotational-translational (R-T) energy exchange that can't be obtained by a physical experiment. Second, it can serve as a test and verification of numerical methods by comparison with existing experimental data. The experimental data for Nitrogen shock structure are obtained by registration of electron beam induced fluorescence [3-6], adsorption of an electron beam [7], and by Raman spectroscopy [8], with the use of jets, wind tunnels, and shock tubes. The most definite experimental conditions were realized for moving shock waves in the tube experiments [7], but the applied method of measurements provided only density profiles. In other experiments with steady shocks formed in expanding free jets and wind tunnels, the thermodynamic equilibrium between rotational and translational modes before the front may be distorted influencing not only the shock wave structure, but also rotational spectrum and rotational temperature as well.

Most computations of the shock wave structure by DSMC method were carried out with application of different phenomenological relaxation models for the internal energy that involve numerous assumptions, some of which are not physically justified [9]. More rigorous Monte Carlo approach that uses classical trajectory calculations of the interactions of rotating molecules [10] requires enormous amount of calculations. More economic DSMC relaxation model based on the trajectory calculations was proposed in [11].

In the present computations the molecular collisions are described by the Lennard-Jones interaction potential with parameters and the rotational spectrum data taken from [12]. The cross sections for the R-T relaxation are calculated according to [13] and are based on molecular dynamic simulations of the collision processes. Simulations are performed in a wide range of Mach numbers (from $M=1.5$ to 10) under experimental conditions of [3-7].

KINETIC EQUATION

The Generalized Boltzmann Equation (GBE) has been obtained in [13] by considering classical interactions of rigid rotors and the application of the quantum mechanics discretisation rules to the obtained continuous energy spectrum. It replaces the Wang Chang –Uhlenbeck Equation (WC-UE) for the case when the internal energy levels of molecules are degenerated. Although the GBE is similar to the WC-UE, it differs from the latter by a factor related to statistical weights of the levels and gives different equilibrium spectrum.

The GBE has the form

$$\frac{\partial f_i}{\partial t} + \xi \frac{\partial f_i}{\partial \mathbf{x}} = R_i, \quad (1)$$

where the collision operator is given by the expression

$$R_i = \sum_{jkl} \int_{-\infty}^{\infty} \int_0^{2\pi} \int_0^{b_m} (f_k f_l \omega_{ij}^{kl} - f_i f_j) P_{ij}^{kl} g b d b d \phi d \xi_j \quad (2)$$

Here f_i is the distribution function for the level i , P_{ij}^{kl} is the probability of the transfer from levels i, j to the levels k, l , and the factor $\omega_{ij}^{kl} = (q_k q_l) / (q_i q_j)$, q_i being the degeneration of the energy level. For simple levels the GBE is reduced to the WC-UE, therefore it can be considered as a more general form of the kinetic equation for molecular gases with internal degrees of freedom. In [1] this equation was obtained directly from WC-UE by grouping q_i single levels that have the same energy and form one degenerated level.

Nitrogen Model

We consider the model of molecular Nitrogen having Lennard-Jones potential (6, 12) with the depth of the potential well of $\varepsilon = 91K$, the degeneration of rotational level $q_i = 2i + 1$, with $i = 0, 1, \dots, \infty$, and the energy of the levels $\varepsilon_i = \varepsilon_{r0} i(i + 1)$, where $\varepsilon_{r0} = 2.9K$. For the transition probabilities we use the formulae given in [13] that are obtained by fitting results of molecular dynamic simulations of rigid rotors that model N_2 molecules

$$P_{ij}^{kl} = P_0 \omega_{ij}^{kl} [\alpha_0 \exp(-\Delta_1 - \Delta_2 - \Delta_3 - \Delta_4) + \frac{1}{\alpha_0} \exp(-\Delta_3 - \Delta_4)] , \quad (3)$$

where

$$\Delta_1 = |\Delta e_1 + \Delta e_2| / e_{tr0}, \quad \Delta_2 = 2 |\Delta e_2 - \Delta e_1| / e_{tot}$$

$$\Delta_3 = 4 |\Delta e_1| / (e_{tr0} + e_i), \quad \Delta_4 = 4 |\Delta e_2| / (e_{tr0} + e_j)$$

$$\Delta e_1 = e_i - e_k, \quad \Delta e_2 = e_j - e_l, \quad \alpha_0 = 0.4 e_{tot} / e_{tr0}$$

$$e_{tr0} = m g^2 / 4, \quad e_{tot} = e_{tr0} + e_i + e_j.$$

The energy conservation law selects transitions with non-zero probability during collision process. From

$$m g_{ij}^2 / 4 + e_i + e_j = m g_{kl}^2 / 4 + e_k + e_l \text{ it follows that } P_{ij}^{kl} > 0, \text{ if } g_{kl}^2 \geq 0, \text{ else } P_{ij}^{kl} = 0.$$

The probabilities should obey the normalization condition $\sum_{k,l} P_{ij}^{kl} = 1$

The elastic collision is a particular case of the collisions. Note, that the formula (3) gives preference to the transitions between close energy levels.

We can separate the molecule interaction process during collisions into two stages. During the first stage, molecules interact in an elastic way according to the molecular potential. This stage determines the deviation angle of the relative velocity. During the second stage the modulus of the relative velocity changes according to the energy conservation equation. The formula (3) is averaged over all interactions and does not depend on the impact parameter. In [2] the inelastic collisions were limited by some impact parameter common for all the interactions. In the presented computations we limited the deviation angle by a value 0.13 below which the R-T transition is prohibited.

Solution Procedure

The kinetic equation (1) is solved by the splitting scheme. For a time step $\tau \ll \tau_0$, where τ_0 is a mean inter collision time, the equation (1) is replaced by the sequence

$$\begin{aligned} \text{a)} \quad & \frac{\partial f_i}{\partial t} + \xi \frac{\partial f_i}{\partial \mathbf{x}} = 0 \\ \text{b)} \quad & \frac{\partial f_i}{\partial t} = R_i \end{aligned}$$

The collision operator R_i is evaluated at a fixed uniform grid S_0 in velocity space by the conservative projection method described in [1, 2]. The equation a) is solved by a second order flux conservative method.

The Problem of Shock Wave Structure

The SW structure is formed as a final stage of the evolution of discontinuity in initial distribution function. The problem is posed at the interval $-L_1 \leq x \leq L_2$ with the discontinuity at $x = 0$. The initial distribution function at both sides presents the equilibrium distribution with respect to velocities and rotational spectrum. It has the form

$$f_i^{1,2}(\xi, x) = n^{1,2} [m / (2\pi T^{1,2})]^{3/2} \exp\left[-\frac{m(\xi - u^{1,2})^2}{2T^{1,2}}\right] \frac{2i+1}{Q_r} \exp\left(-\frac{e_i}{T^{1,2}}\right)$$

Here Q_r is the statistical sum, parameters $(n, T, u)^{1,2}$ are defined by the Rankin-Hugoniot relations with $\gamma = 7/5$. At the boundaries of the computational domain this function is kept constant.

The number of levels was selected based on the temperature range of the considered problem.

RESULTS OF SIMULATIONS

We have simulated the shock wave (SW) structure in Nitrogen for a wide range of Mach numbers and compared with experimental cases of [7] for $M = 1.53, 1.7, 2, 2.4, 3.2, 3.8, 6.1, 8.4, 10$ and [3-5] for $M=7$ and $M=12.9$. For the first 6 Mach numbers we've obtained the density profiles coincided with [7], and for other cases results were close.

Figure 1 compares the data of [7] with simulation results for $M=1.53$ and $M=1.7$. The computations were performed using 30 rotational levels for the first case and 32 levels for the second case. Our results for $M=1.7$ are in better agreement with computations of Koura [10] than with experiment [3] and give the rotational temperature profile preceding the density profile, whereas in the experiment the second graph goes slightly ahead of the first one.

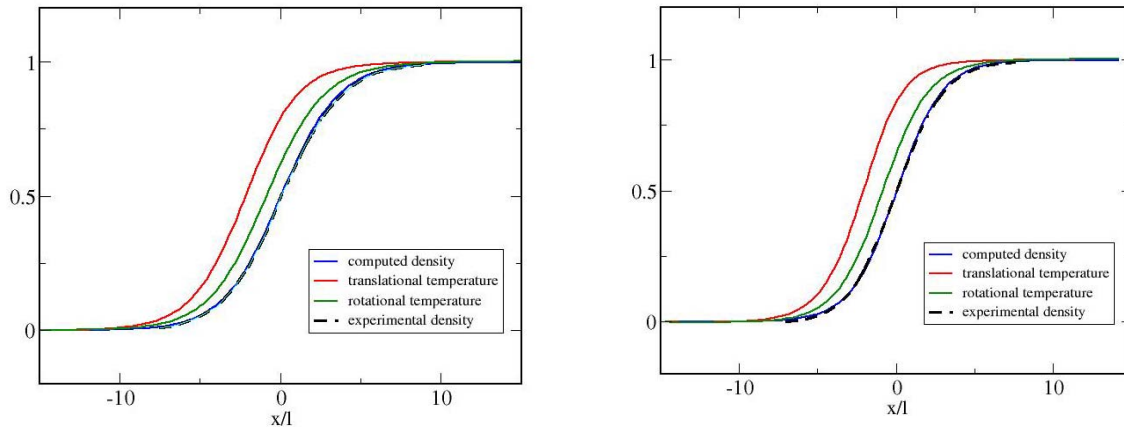


FIGURE 1. Shock wave structure in Nitrogen for $M=1.53$ (left) and $M=1.7$ (right)

The typical CPU time was about 35 hours in both cases on an AMD64 3000 processor.

Figure 2 shows rotational spectrum for $M=3.2$ calculated with 44 rotational levels at several points along the wave front: $x = -\infty$, $x = x_c - 2\lambda$, $x = x_c - \lambda$, $x = x_c$, $x = x_c + \lambda$, $x = \infty$. Here x_c denotes the SW center defined as the point where the reduced gas density is equal to $1/2$. On the x -axes is the number of the rotational level, on the y -axes is the population of the r -th rotational level. It is seen that some peculiarity of the spectrum around 7-8 levels is observed at the second, third and fourth spatial positions.

This deviation from equilibrium spectrum is better seen on the right part of Figure 2 where the population of the rotational level is plotted in coordinates $y = \ln \frac{n_r}{(2r+1)n}$, $x = \varepsilon_r = r(r+1)\varepsilon_{r0}$, where n_r is the population of the r -th level, $n = \sum_{r=0}^{\infty} n_r$ is the gas density at the given point, ε_r is the energy of the level, and ε_{r0} is the rotational energy quantum. The density and temperature are normalized by their left side values. The equilibrium degenerated distributions

$$n_r = \frac{2r+1}{n} \exp(-\varepsilon_r / T)$$

at the SW boundaries are represented by straight lines in these coordinates. It is seen in Figure 2 that the rotational spectrum deviates from the equilibrium spectrum inside the SW, in agreement with experimental data [5]. The most noticeable deviation occurs at the second point. In the center of the wave front and on the right part of the SW, the deviation is considerably smaller. Note, that in the middle part the spectrum doesn't present a "mixture" of the left side and the right side spectral distributions that confirm the experimental observation of [6].

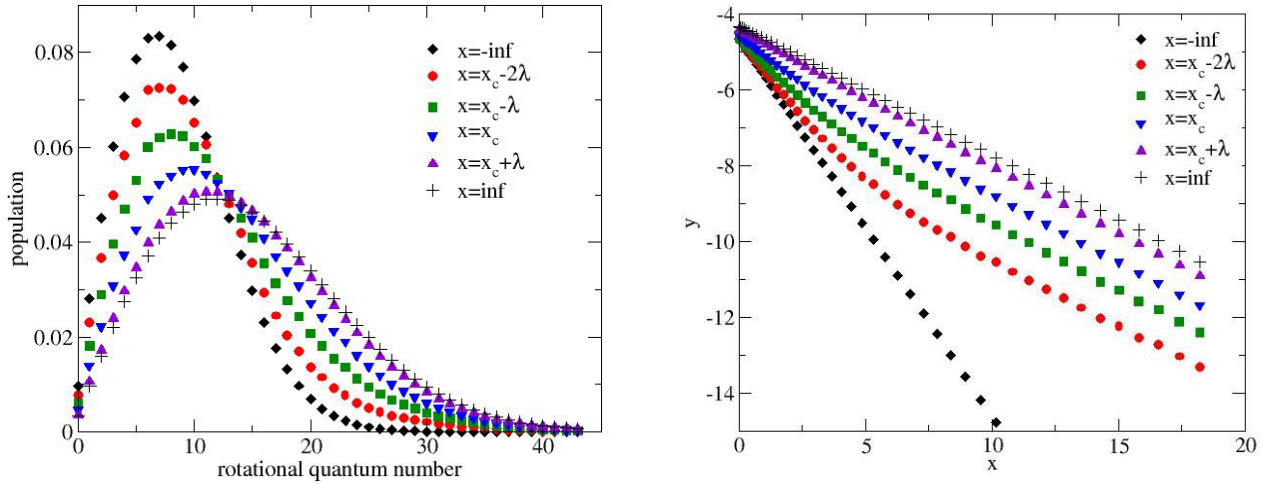


FIGURE 2. Rotational spectrum at different points of the shock wave at $M=3.2$.

Figure 3 (left part) shows distributions of gas density, translational and rotational temperatures obtained in our simulations for $M=12.9$ for the experimental conditions of [3]. The right part of Figure 3 shows rotational spectrum for 26 levels at several points along the wave front. The center of SW is located at $x=0$. On the x -axes is the rotational level number; on the y -axes is the population of the rotational levels. It is clearly seen that the rotational equilibrium inside the SW doesn't exist for this high Mach number. Our results are in good agreement with the experimental data of [3] and computations of [10].

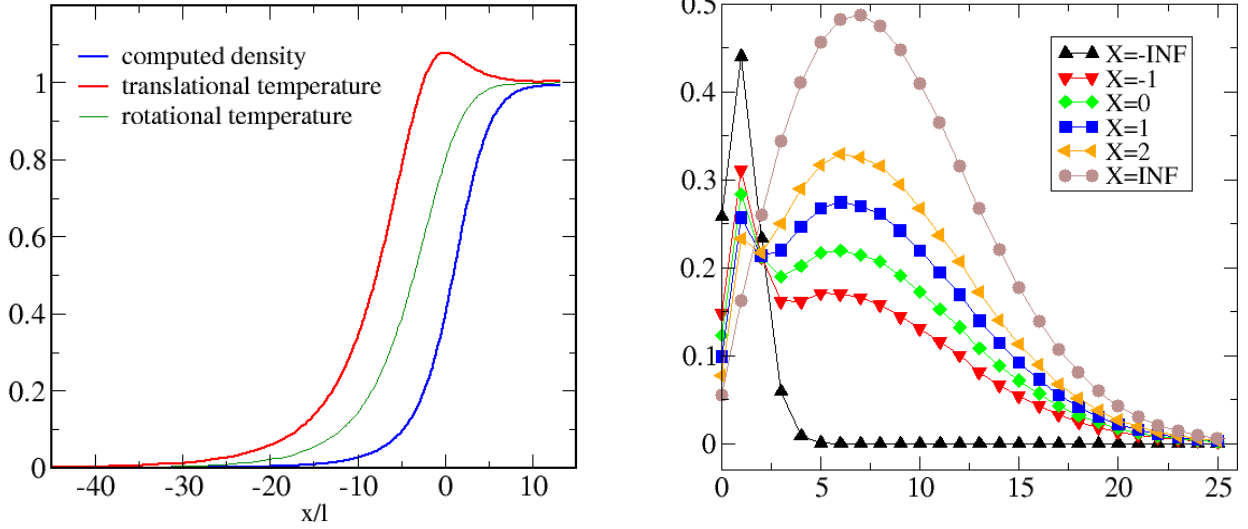


FIGURE 3. Shock wave structure (left) and rotational spectra at different points along the shock wave (right) in Nitrogen at $M=12.9$.

The computations of high-speed flows require using reduced number of “effective” rotational levels. The reduction of the number of the levels is obtained by increasing the rotational quantum ε_0 . The results of computations of SW structure at $M=10$ and room temperature with 16 rotational levels and comparison with the results of [7] are shown in Figure 4, left. It is seen that the longitudinal temperature T_{xx} is about twice larger than the translational temperature, therefore the R-T transitions may occur with much higher kinetic energies that are estimated in some phenomenological models based on the translational temperature. In the right part of the figure the variation of relative populations n_r/n of some levels inside the shock wave is presented. One may notice decreasing populations for the ground and the first excited levels. The populations for other levels rise, but the rise of higher level populations begins with some delay. This may indicate on the cascade character of the R-T process in which the rotational quantum passes from the low energy levels to the high energy ones.

Some numerical tests that justify the use of coarse mesh in velocity space, sometimes exceeding the mean thermal velocity, were performed as well. The use of “efficient” levels and of coarse mesh in velocity space allows considerably reducing the CPU time.

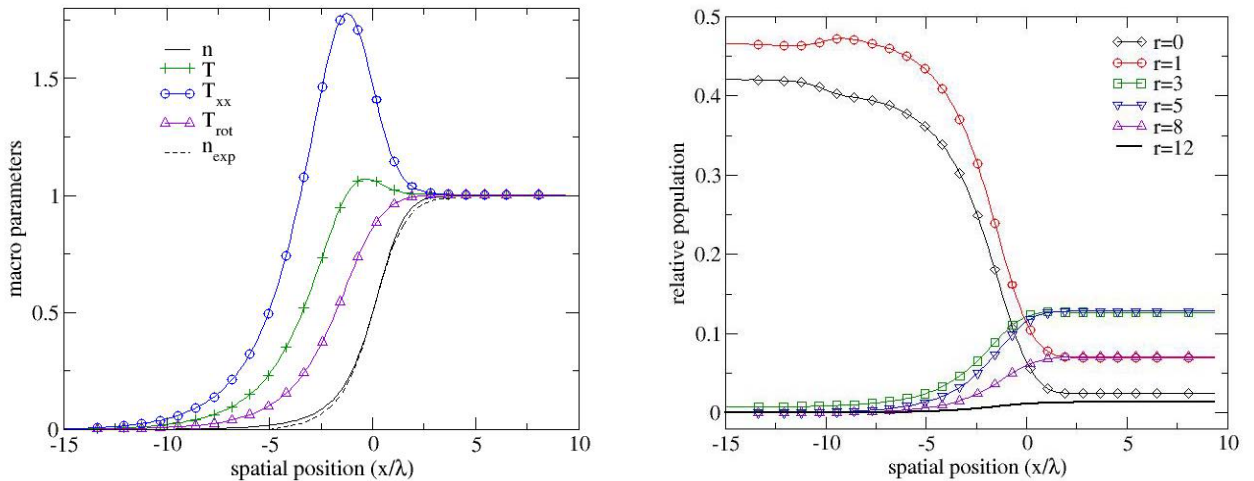


FIGURE 4. Shock wave structure in Nitrogen at $M=10$ for reduced number of “effective” levels.

CONCLUSION

We have simulated the shock wave structure in Nitrogen for Mach number ranging from 1.53 to 12.9 with realistic physical parameters by numerical solution of the generalized Boltzmann equation. No artificial assumptions and simplifications that were not justified from the viewpoint of computational mathematics have been made.

Detailed distributions of gas density, translational and rotational temperatures are obtained together with the rotational spectrum and its variation inside the shock wave front. The computed results are free from the statistical noise typical to Monte Carlo methods. The results of simulations are in good agreement with the experimental data and computations by the advanced Monte Carlo method that uses trajectory calculations of molecular interactions.

The rotational spectrum inside the SW is close to equilibrium for $M < 2.5$, but considerably deviates from equilibrium for strong shocks making the application of phenomenological models quite dubious in the last case. The kinetic temperature profiles for strong SW exhibit a noticeable overshoot. The longitudinal temperature is much higher than the kinetic temperature. For all Mach numbers, the profiles of the rotational temperature are monotonous and are located between the kinetic temperature and density profiles.

The applied method is economic in arithmetic operations because the most consuming calculations of the post collision velocities and of the normalized probabilities of the R-T transitions are made in advance and then applied for all nodes in physical space. Despite this, calculations require considerable CPU time that can be reduced by using crude discretization of the velocity space and of the rotational energy spectrum.

ACKNOWLEDGMENTS

The work was supported by the US Air Force SBIR Project F33615-03-M-3326. The work of F.G.Tcheremissine was also supported by the Russian Foundation for Basic Research under grant 04-01-00347, and by the Program 03 of Mathematical Department of the RAS.

REFERENCES

1. F.G. Cheremisin, Solution of the Wang Chang – Uhlenbeck Master Equation. Doklady Physics, 2002, V. 47. N. 2. pp. 872-875.
2. F.Tcheremissine, Direct Numerical Solution of the Boltzmann Equation, Rarefied Gas Dynamics, 24-th Intern. Symp. on RGD. M.Capitelli ed., AIP Conf. Proceedings 762, Melville, New York, 2005, pp. 677-685.
3. F. Robben and L. Talbot, Measurements of Shock wave Thickness by the Electron Beam Fluorescence Method, Phys. Fluids, 1966, V.9, N.4, pp. 633-643.
4. F. Robben and L. Talbot, Measurements of Rotational Temperatures in a Low Density Wind Tunnel, Phys. Fluids, 1966, V.9, N.4, pp. 644-652.
5. F. Robben and L. Talbot, Experimental Study of the Rotational Distribution Function of Nitrogen in a Shock Wave, Phys. Fluids, 1966, V.9, N.4, pp. 653-662.
6. R.B.Smith, Electron-Beam Investigation of a Hypersonic Shock Wave in Nitrogen, Phys.Fluids, 1972, V.13, N.6, pp. 1010-1017.
7. H. Alsmeyer, Density profiles in argon and nitrogen shock waves measured by the absorption of an electron beam, J. Fluid Mech., 1976, V.74, part 3, pp.497-513.
8. A.Ramos, B.Mate, G.Tejada, J.M.Fernandes, and S.Montero, Raman spectroscopy of hypersonic shock waves. Phys. Rev., 2000, V.62, N.4, pp. 4940-4945.
9. I.G.Wysong and D.C.Wadsworth, Assessment of direct simulation Monte Carlo phenomenological rotational relaxation models, Phys.Fluids, 1998, V.10, N.11, pp.2983-2994.
10. K.Koura, Direct simulation Monte Carlo study of rotational nonequilibrium in shock wave and spherical expansion of nitrogen using classical trajectory calculations. Phys.Fluids, 2002, V.14, N.5, pp.1689-1695.
11. T.Tokumasu and Y.Matsumoto, Dynamic molecular collision (DMC) model for rarefied gas flow simulations by the DSMC method, Phys.Fluids, 1999, V.11, N.7, pp.1907-1920.
12. J.O. Hirschfelder, Ch. F. Curtiss, R.B. Bird, Molecular Theory of Gases and Liquids, John Wiley and Sons, inc., N.-Y., Chapman and Hall, London, 1954.
13. A.A. Beylich, An Interlaced System for Nitrogen Gas. Paper presented at a workshop on CECAM, ENS de Lyon, France, 2000.